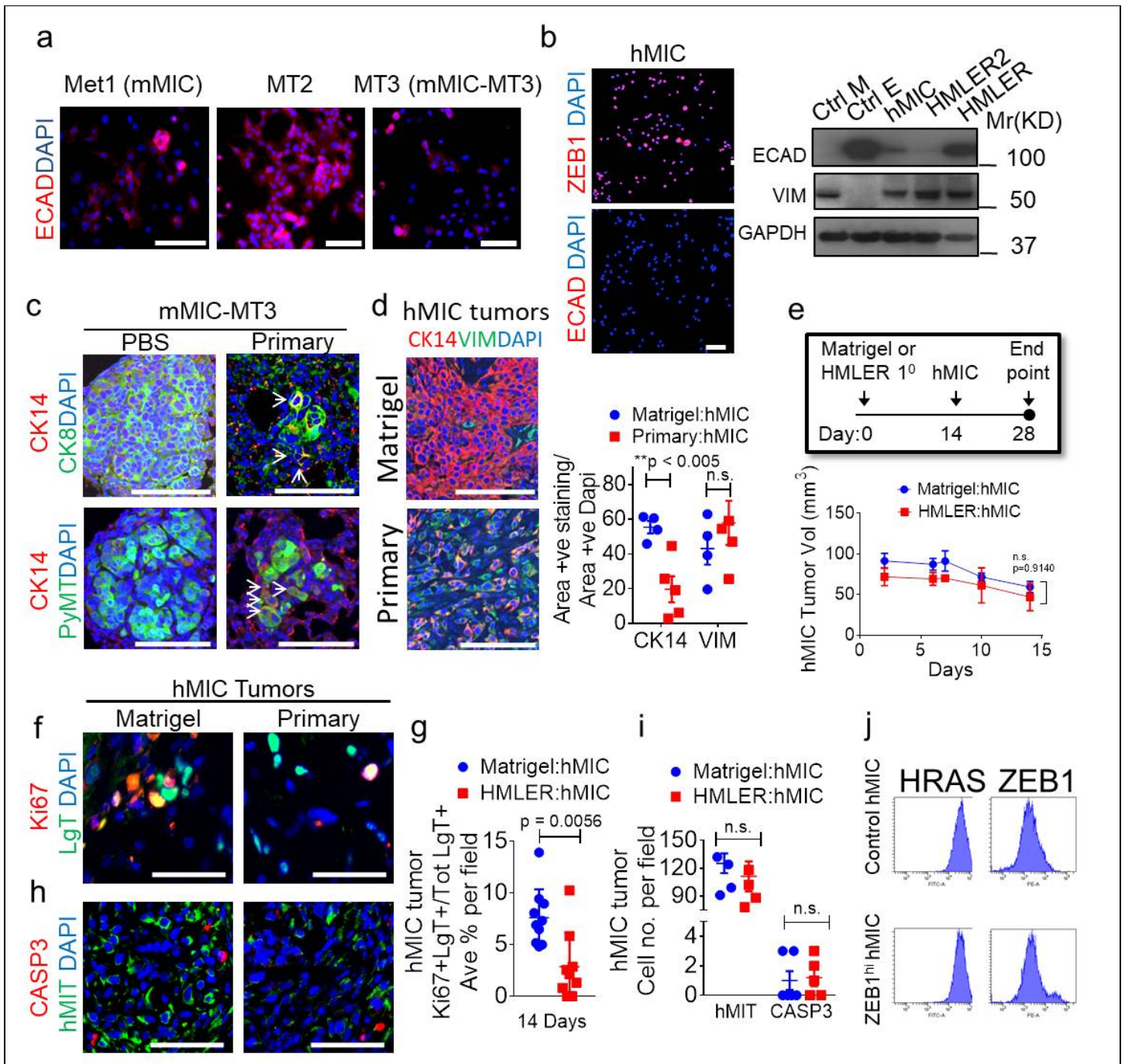


Supplementary Figure 1

Primary tumors inhibit outgrowth of distant metastasis-initiating cells

**a**, Met1 orthotopic primary tumor growth kinetics, FVB mice, represented in Fig. 1b (n=10). **b**, Schematic of sequential subcutaneous experimental model (left) and growth kinetics (right) of Met1 secondary tumors ( $2.5 \times 10^5$ /mouse; implanted at day 14) in mice with PBS control or Met1 primary tumor ( $2.5 \times 10^5$ /mouse; n=5 animals/cohort). **c**, Numbers of pulmonary macrometastases following tail vein injection of MT2 or MT3 cells ( $7.5 \times 10^5$  cells/mouse; n=3). Macrometastases >100 microns were quantified on microscope tissue sections from 4 lung lobes per mouse. **d**, Met1 orthotopic tumor growth kinetics, Nude mice, represented in Fig. 1f (n=5). **e**, Schematic of experimental model (left), and number of pulmonary macrometastases following tail vein injection of  $2.5 \times 10^5$  hMICs into Nude mice with either Matrigel (n = 10) or HMLER primary tumors (n=9; original injection of  $5.0 \times 10^5$  cells/mouse) (right). Macrometastases (>100 microns) or micrometastases (>5 cells or <5 cells) were quantified from microscopic whole lung tissue sections. **f**, Schematic of experimental model (applies to g and h). **g**, Growth kinetics of HMLER primary tumors, Nude mice, described in Figure 1h (n=10). **h**, MIC-231 tumor growth kinetics, Nude mice, opposite Matrigel control (n=12) or HMLER primary tumors (n=5). Representative of 2 experiments. **i**, Images: representative immunofluorescent images of 231-MIC tumors grown opposite Matrigel control or an HMLER primary tumor (represented in Supplementary Fig. 1h) stained with Ki67 (red), hMIT to identify human mitochondria (green), DAPI (nuclei, blue); Scale bars=100  $\mu$ m. Graph: Quantification of Ki67+hMit+ cells as a percentage of the total number of hMit+ tumor cells/microscopic field (n=9 images; 3 tumors/cohort). Source data for **a**, **b**, **c**, **d**, **e**, **g**, **h**, **i** in Supplementary Table 1. 2-way ANOVA, followed by Sidak's multiple comparison test (**b**, **g**, **h**); 1-sided Welch's t test (**e**); 2-sided Welch's t test (**c**, **i**).

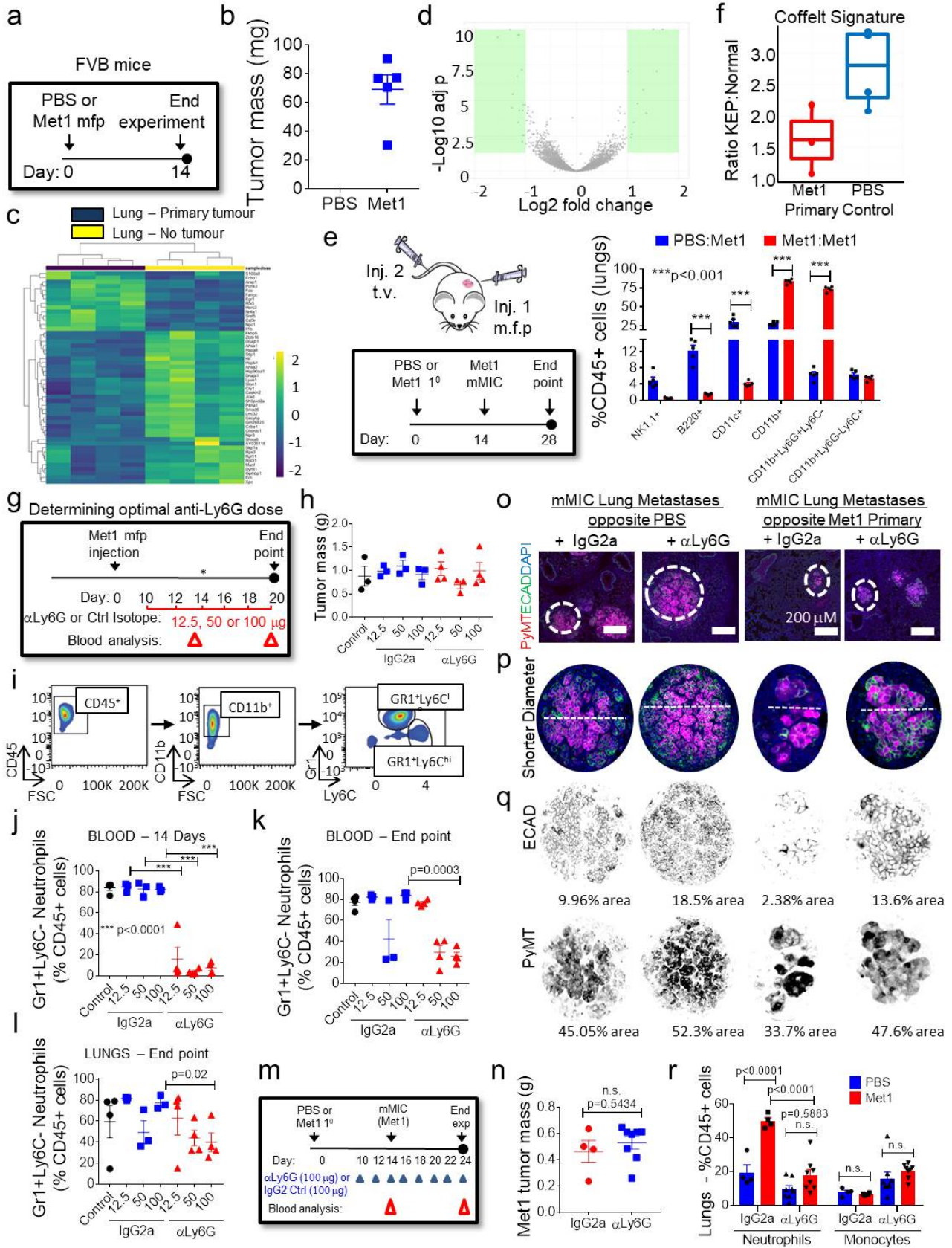


Supplementary Figure 2

### MIC Differentiation is Perturbed by the Presence of a Primary Tumor

**a**, In vitro immunocytochemical fluorescence showing E-cadherin (ECAD, red) and DAPI (nuclei, blue) in Met1 parental cell line (mMIC) and Met1-derived clones, MT2 and MT3 (mMIC-MT3). **b**, Images: Immunofluorescence showing ZEB1 and ECAD expression in cultured hMICs prior to xenotransplantation. Western blot: mesenchymal marker Vimentin (VIM) and epithelial marker ECAD protein in polyclonal HMLER cells and derivative hMIC and HMLER2 cells. GAPDH shown as internal control. Positive controls: Ctrl E (epithelial-MCF7Ras); Ctrl M (mesenchymal CD44<sup>hi</sup> HMLER cells). **c**, Merged immunofluorescent images of mMIC-MT3 tumors (described in Fig. 1d) stained for basal cytokeratin 14 (CK14, red), luminal CK8 (green) or PyMT antigen (expressed by tumor cells only-green). Arrows - CK14+ tumor cells. **d**, Images: hMIC tumors (from Fig 1i) stained with CK14 (red), VIM (green) and DAPI (blue); Graph: quantification of indicated

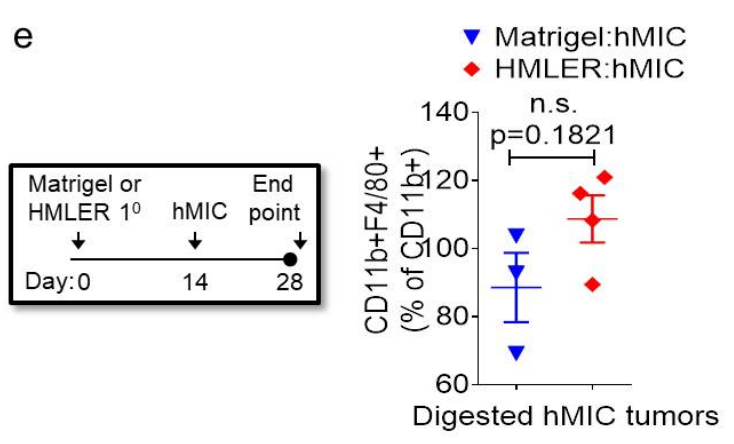
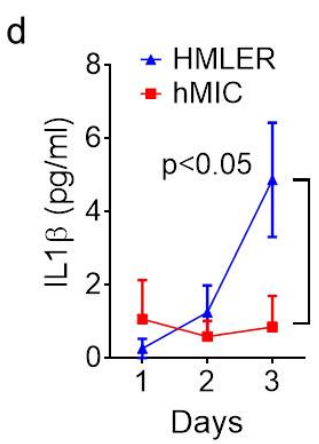
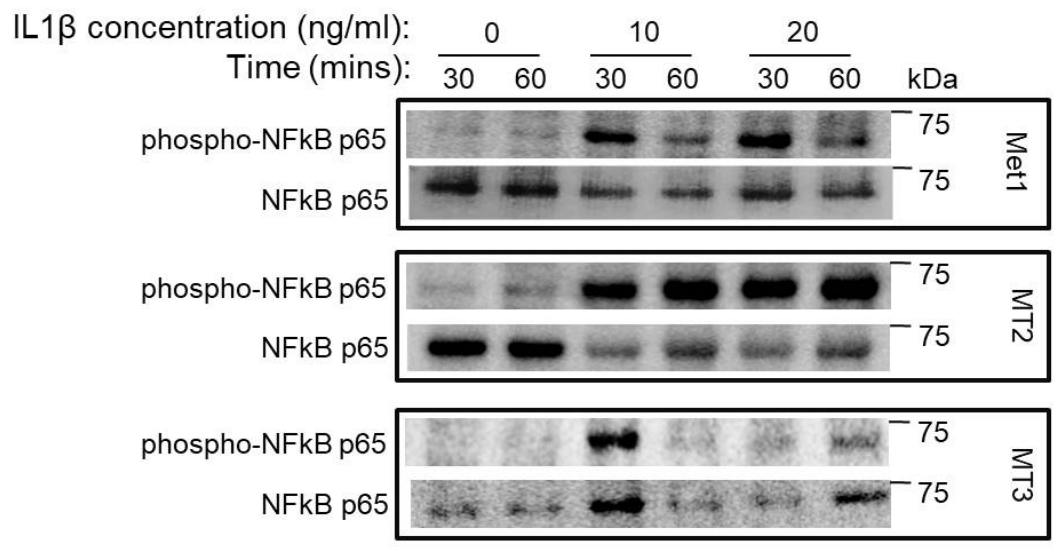
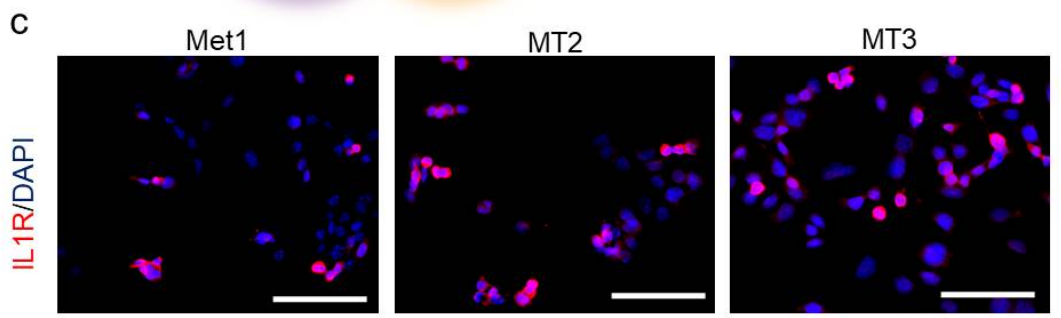
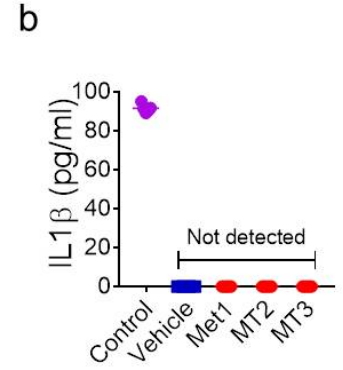
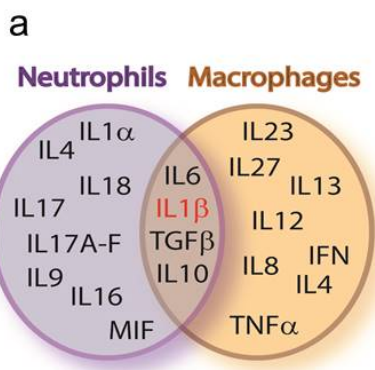
stains on hMIC tumors grown opposite Matrigel (n=4) or primary tumor (n=5). **e**, Schematic: modeling early stages of hMIC colonization. Graph: hMIC tumor growth kinetics opposite Matrigel control or HMLER primary tumor (n=4/group); differences not statistically significant. **f, g**, Immunofluorescent images (**f**) and quantification (**g**) of hMIC tumors stained for ki67 (red), LgT antigen (tumor cells, green), and DAPI (nuclei, blue) as a percentage of total LgT+ cells. Control, n=10 images, 4 tumors; HMLER cohort, n=9 images, 4 tumors. **h, i**, Immunofluorescent images (**h**) and quantification (**i**) of staining hMIC tumors for cleaved caspase3 (CASP3, red), human-specific mitochondria (hMIT, green), and DAPI (nuclei, blue) grown in mice with Matrigel control (n=6 images, 4 tumors) or HMLER primary tumors (n=5 images, 4 tumors). **j**, Expression of ZEB1 (ZEB1-GFP construct) or HRAS (HRAS-tomato construct) analyzed by FACS ( $1.0 \times 10^5$  cells) in Control hMIC or ZEB1<sup>hi</sup> hMIC (from Fig. 2n-p). All scale bars=100  $\mu$ m. Source data for **d, e, g, i** in Supplementary Table 1 and **d** on Supplementary Figure 9. 2-way ANOVA (**e**); 2-sided Welch's t test (**d, i**); 2-sided Mann-Whitney test (**g**).



## Supplementary Figure 3

### Innate Inflammatory Cells are Necessary for MIC Colonization

**a**, Experimental schematic for tissues used for RNA-seq analysis (Fig. 3a-c and Supplementary Fig. 3b-e). **b**, Met1 primary tumor mass in FVB mice (n=5). **c, d**, RNA-seq analysis on lungs from mice with PBS control (n=4) or a Met1 primary tumor (n=4). Heatmap (**c**): top 50 differentially expressed genes (by adjusted p-value, DESeq2). Blue=low, green=mean, and yellow=high relative expression levels. PBS control lungs (yellow), Met1 primary tumor-bearing lungs (purple). Volcano plot (**d**): DESeq2 comparison Single gene with  $P_{adj} < 0.05$  and absolute  $\log_2(\text{FoldChange}) > 1$  (green). **e**, Experimental schematic and flow cytometric quantification of immune cell populations in lungs of indicated FVB mice at 28-day end point (see Fig. 1a). **f**, Ratio of genes expressed by pro-metastatic immunosuppressive neutrophils from *K14cre;Cdh1F/F;Trp53F/F* (KEP) mice to control neutrophils from wild type littermates (KEP:Normal)<sup>13</sup> extrapolated onto our signatures from control (blue) primary tumor-bearing lungs (red). Higher ratios indicate higher pro-metastatic KEP signature. Box plot is median, 25<sup>th</sup> and 75<sup>th</sup> percentiles; whiskers extend to minimum and maximum values. **g**, Experimental design to identify optimal anti-Ly6G dose for neutrophil depletion. **h**, Primary tumor mass in Control anti-IgG2a (n=3 mice/cohort) and anti-Ly6G (n=4 mice/cohort). **i**, Flow cytometric gating strategy for neutrophils (CD45+CD11b+Gr1+Ly6Clo) and monocytes (CD45+CD11b+Gr1+Ly6Chi). **j-l**, Flow cytometric analysis of blood at 14d (**j**), 20d (**k**), and lungs 20d (**l**) in experiment described in (**g**). Control anti-IgG2a n=3 mice/cohort; anti-Ly6G n=4 mice/cohort. **m**, Schematic modeling neutrophil depletion experiment (**n-r**). **n**, Primary tumor mass represented in Fig. 3i (control IgG2a n=4 mice/cohort; anti-Ly6G n=8 mice/cohort). **o**, Immunofluorescent images of Met1 lung metastasis. Scale bars= 200  $\mu\text{m}$ . **p**, Metastases at higher magnification (indicated in circles in (**o**)) analyzed by ImageJ to measure shortest-length diameter). **q**, Single channels of ECAD and PyMT staining measured by ImageJ analysis (Fig. 3k, l). **r**, End point flow cytometric analysis of neutrophils and monocytes in lungs of mice treated with control IgG2a (n=4 mice/cohort) or anti-Ly6G (n=8 mice/cohort). Source data for **b, e, h, j, k, l, n, r** in Supplementary Table 1. DESeq2's Wald test two-sided (**c**); 2-sided Welch's t-test (**f**); 2-sided Welch's t test (**n**); 2-way ANOVA followed by Sidak's multiple comparison test (**f, h, j, k, l, o**).

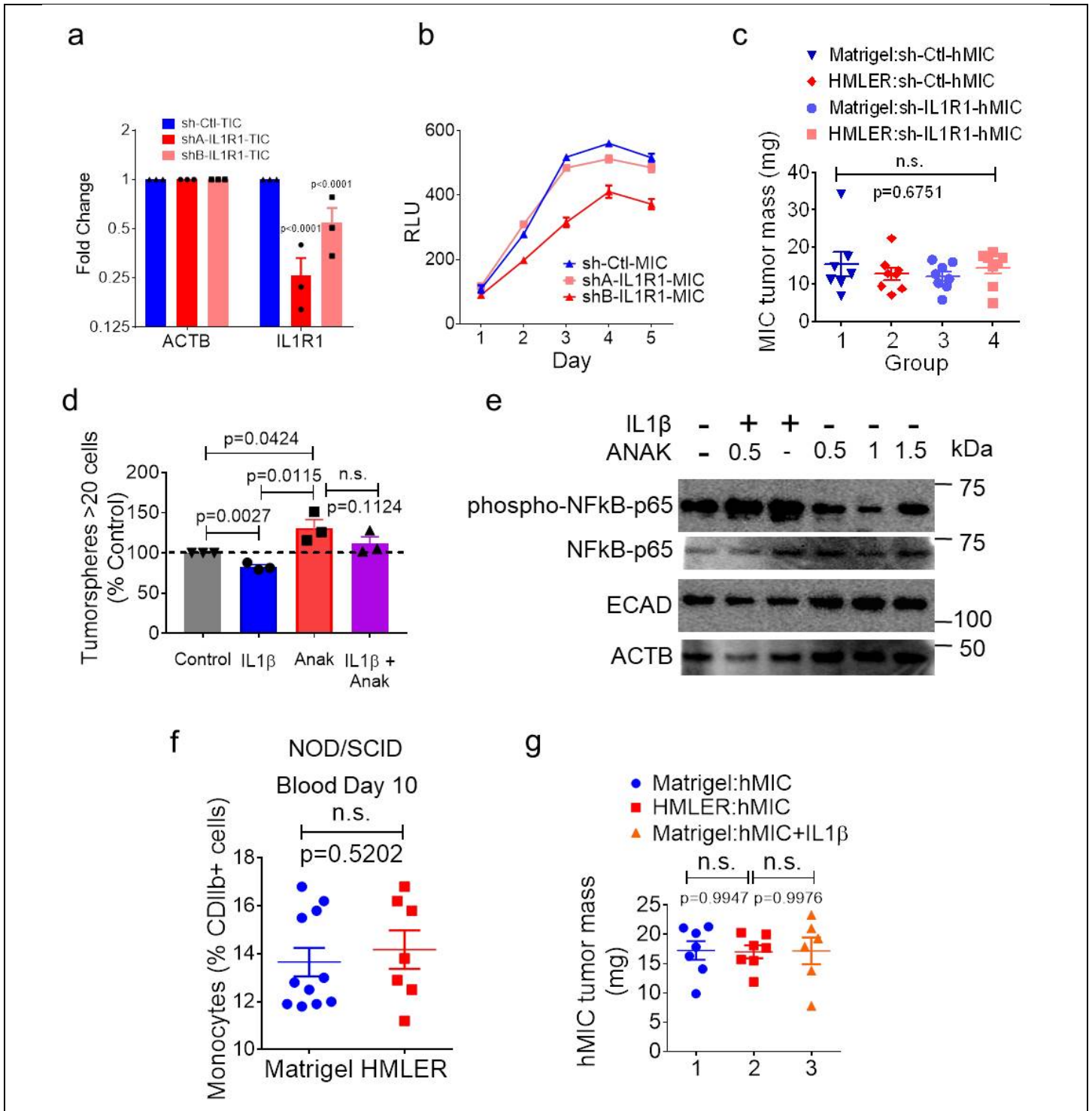


## Supplementary Figure 4

### Innate Inflammatory Response is sufficient for MIC colonization

**a**, Some of the predominant cytokines expressed by monocytes, neutrophils or by both. **b**, ELISA to detect cumulative IL-1 $\beta$  in the conditioned media of Met1 cell line and its derived clones after 3 days *in vitro* (n=5/group). **c**, Met1 parental cells and the MT2 and MT3 subclones stained as indicated (upper panel). Scale bars=100  $\mu$ m. Western blot detecting phospho-NF $\kappa$ B p65 (activated form of NF- $\kappa$ B p65) or total NF- $\kappa$ B p65 (NF $\kappa$ B p65) in Met1, MT2 and MT3 treated *in vitro* with indicated doses of IL-1 $\beta$  at indicated time points (lower panel). **d**, ELISA to detect cumulative IL-1 $\beta$  in the conditioned media of HMLER and hMIC cell lines over 3 consecutive days of *in vitro* culture (n=4/group). **e**, Experimental schematic and flow cytometric quantification of immune cell populations in digested hMIC tumors from indicated cohorts in Nude mice at the 28-day experimental end point (see Fig. 2i) (n=3 in Matrigel control and 4 in HMLER cohort). Source data for **b**, **d**, **e** in Supplementary Table 1. 2-sided Welch's t test (**b**, **e**); Two-way ANOVA, Sidak's multiple comparisons test (**d**).





Supplementary Figure 5

**IL-1R1 Pathway is sufficient to block MICs colonization**

**a**, qRT-PCR to determine *IL-1R1* mRNA levels in hMIC expressing shRNA against IL-1R1 (shA-IL-1R1-MIC and shB-IL-1R1-MIC) compared to hMIC expressing a scrambled shRNA (sh-Ctl-MIC). B-actin (ACTB) served as the internal control (n=3, average technical triplicates). **b**, Proliferation analysis (CyQuant assay) comparing growth of MIC-control cells to those expressing shRNA against IL-1R1 (shA-IL-1R1-MIC and shB-IL-1R1-MIC; n=3 in triplicate representative of 5 independent experiments). **c**, hMIC tumor mass (mg) at the

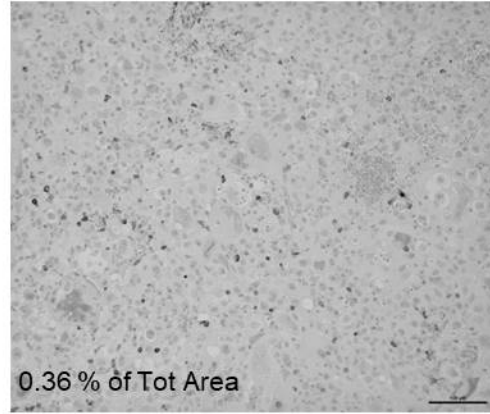
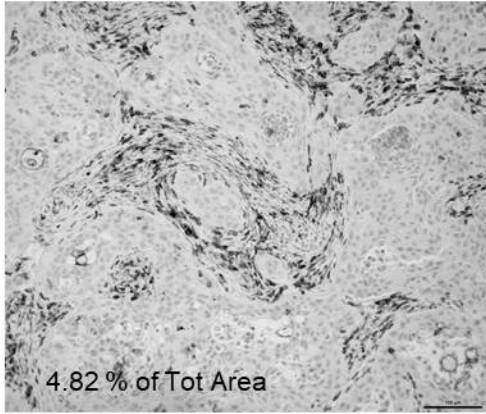
4-week experimental end point (n=8/cohort, except sh-Ctl-MIC n=7). **d**, Met1 tumorspheres generated in 3 independent experiments, treated with IL-1 $\beta$  (10 ng/mL), Anakinra (500 ng/ml) or IL-1 $\beta$  + Anakinra combination (n=3 replicates, 28 technical replicates). **e**, Western blot detecting phospho-NF $\kappa$ B p65, total NF $\kappa$ B p65, or ECAD in Met1 cells treated with 10ng/ml of IL-1 $\beta$  and increasing doses of ANAKINRA (IL-1Ra) for 48h. B-actin (ACTB) was used as a loading control. **f**, Flow cytometric analysis of monocytes (CD11b<sup>+</sup>Ly6C<sup>+</sup>Ly6G<sup>lo</sup>) presented as % CD11b<sup>+</sup> cells in blood at 10 days, prior to the injection of contralateral tumors (Matrigel n=11 (combined from Groups 1 and 3); HMLER n=7). **g**, Final mass (mg) of hMIC tumors from indicated cohorts (differences not statistically significant, Control n=7, HMLER n=6 mice/group). Representative of 1 experiment. Source data from **a, b, c, d, f, g** in Supplementary Table 1. 2-way ANOVA and Sidak's multiple comparisons test (**a, b**); 1-way ANOVA (**c, g**); 2-sided Student's t tests (**d**); 2-sided Mann-Whitney test (**f**).

a

HMLER

HMLER2

ImageJ Analysis



**Supplementary Figure 6**

**Primary tumors induce an inflammatory response**

a, Representative images of F4/80 staining and ImageJ analysis used to quantify area covered by positive F4/80 staining in Figure 6b. Scale bar=100  $\mu$ m.

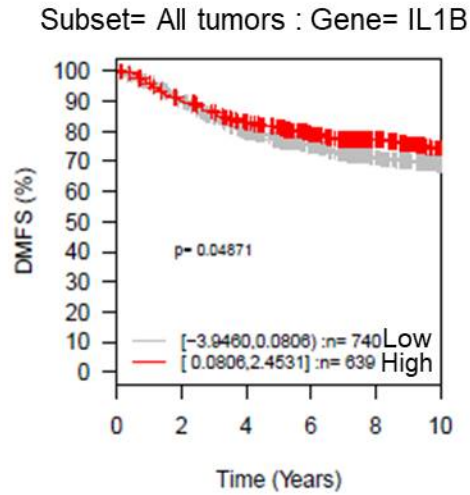


## Supplementary Figure 7

### Inhibition of IL-1R1 at Primary Tumor Site Enables MIC Colonization

**a**, KEGG IL-17 signaling pathway (mmu04657). The log<sub>2</sub> fold change values comparing primary tumor to control lungs. Red, higher expression in primary tumors; green, higher expression in normal lungs (n=3 for Met1 primary tumors, and n=4 control lungs). **b**, Inflammatory cytokine array analysis of conditioned media from HMLER and hMIC cells after 3 days in culture (n=2 biological replicates, 3 technical replicates). Results are fold change (Log<sub>2</sub>) HMLER/MIC. **c**, Mouse inflammatory cytokine array results from plasma of mice bearing Matrigel control, HMLER, or HMLER+IL-1Ra tumors after 2 weeks in vivo (n=2, plasma pooled from 3 individual animals per sample). **d**, hMIC tumor mass (4 weeks) grown opposite Matrigel control (n=8), HMLER primary tumor (n=7), or HMLER+IL-1Ra antagonist (IL-1Ra) (n=8). Representative of 1 experiment. **e**, Graph: HMLER primary tumor mass embedded in control Matrigel (n=5) or Matrigel with 100ng/ml IL-1Ra (n=6). Incidence (%) marked on graphs. **f**, Hematoxylin and eosin (H&E) stains from HMLER and HMLER+IL1Ra tumors (Figure 7c-g), low and high magnification. **g**, F4/80 staining and ImageJ analysis to quantify area covered by F4/80+ staining in Figure 7e. Boxes indicate area shown in Figure 7e. **h**, Immunohistochemistry showing macrophage infiltration (F4/80 stain) in hMIC tumors grown opposite Matrigel control, HMLER, or HMLER+IL-1Ra primary tumors. **i**, **j**, Photomicrographs of hMIC tumors grown opposite Matrigel control, HMLER primary tumor, or HMLER + IL-1Ra primary tumors. ECAD (red), LgT (green – to detect human tumor cells), DAPI (blue). **(h)** ZEB1 (red), LgT (green), DAPI (blue). Boxes indicate area shown in Figure 7f-g. Scale bars=100 μm. Source data for **b**, **c**, **d**, **e** in Supplementary Table 1. DESeq2's Wald test two-sided (**a**); 2-sided Mann-Whitney test (**d**); 2-sided Welch's t test (**e**).

a

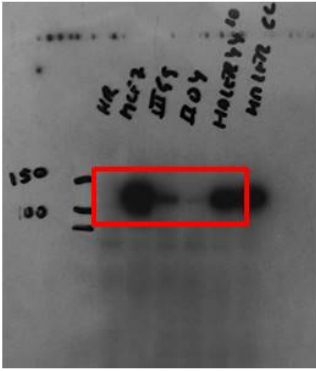


**Supplementary Figure 8**

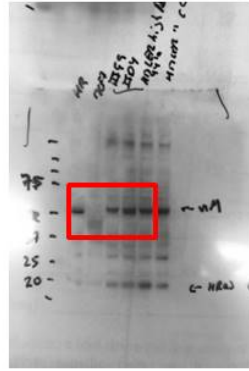
**Analysis of IL1 pathway components as predictors of disease outcome in clinical breast cancer specimens**

a, Kaplan-Meier analysis using distant metastasis-free survival (DMFS) as end point with 10-year censoring based on stratification of *IL1B* gene expression (log<sub>2</sub>; low, grey line, n=740; high, red line, n=639) in tumor tissue from 1,379 breast cancer patients. Logrank p value is shown. Analysis performed using the GOBO database (<http://co.bmc.lu.se/gobo/gsa.pl>).

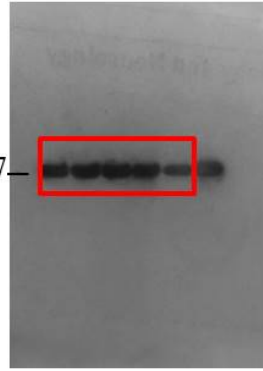
Suppl. Fig. 2b, CDH1



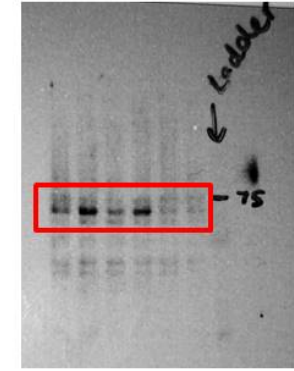
Suppl. Fig. 2b, VIM



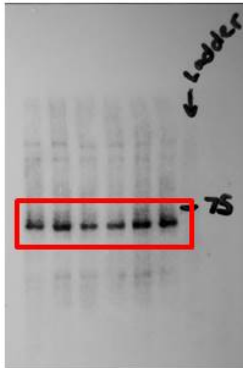
Suppl. Fig. 2b, GAPDH



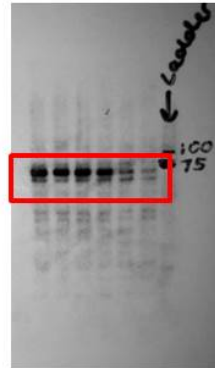
Suppl. Fig. 4c, Met1 P-P65



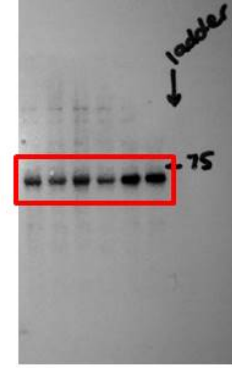
Suppl. Fig. 4c, Met1 Total-P65



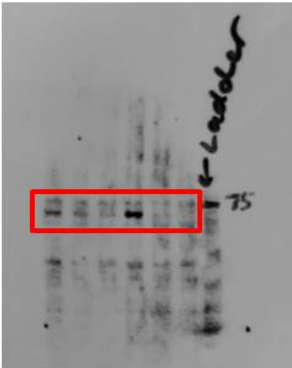
Suppl. Fig. 4c, MT2 P-P65



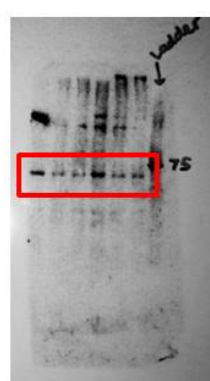
Suppl. Fig. 4c, MT2 Total-P65



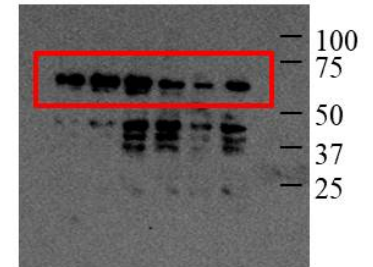
Suppl. Fig. 4c, MT3 P-P65



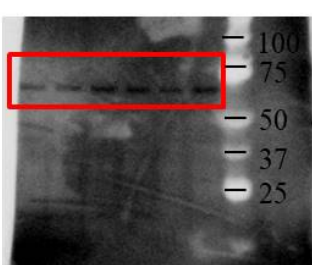
Suppl. Fig. 4c, MT3 Total-P65



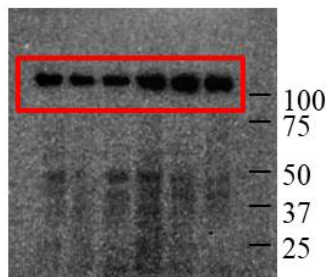
Suppl. Fig. 5e, P-P65



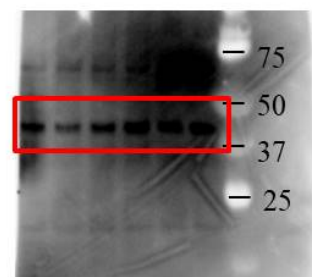
Suppl. Fig. 5e, Total-P65



Suppl. Fig. 5e, CDH1



Suppl. Fig. 5e, ACTB



**Supplementary Figure 9**

**Western blot scanned films**

Boxes highlight lanes used in figures.